

ANRCP-1998-22  
December 1998

# Amarillo National Resource Center for Plutonium

A Higher Education Consortium of The Texas A&M University System,  
Texas Tech University, and The University of Texas System

## Experimental Study of Highly Viscous Impinging Jets

**RECEIVED**

**JAN 08 1999**

Michael Gomon  
Department of Mechanical Engineering  
The University of Texas  
Austin, Texas 78712

**OSTI**

DISTRIBUTION OF THIS DOCUMENT IS UNLIMITED

**MASTER**

Edited by

Angela L. Woods  
Technical Editor

600 South Tyler • Suite 800 • Amarillo, TX 79101  
(806) 376-5533 • Fax: (806) 376-5561  
<http://www.pu.org>

## DISCLAIMER

This report was prepared as an account of work sponsored by an agency of the United States Government. Neither the United States Government nor any agency thereof, nor any of their employees, makes any warranty, express or implied, or assumes any legal liability or responsibility for the accuracy, completeness, or usefulness of any information, apparatus, product, or process disclosed, or represents that its use would not infringe privately owned rights. Reference herein to any specific commercial product, process, or service by trade name, trademark, manufacturer, or otherwise does not necessarily constitute or imply its endorsement, recommendation, or favoring by the United States Government or any agency thereof. The views and opinions of authors expressed herein do not necessarily state or reflect those of the United States Government or any agency thereof.

## **DISCLAIMER**

**Portions of this document may be illegible in electronic image products. Images are produced from the best available original document.**

**ANRCP-1998-22**

**AMARILLO NATIONAL RESOURCE CENTER FOR PLUTONIUM/  
A HIGHER EDUCATION CONSORTIUM**

A Report on

**Experimental Study of Highly Viscous Impinging Jets**

by  
Michael Gomon, B.S.M.E.  
Department of Mechanical Engineering  
The University of Texas  
Austin, TX 78712

Submitted for publication to

**Amarillo National Resource Center for Plutonium**

December 1998

Dedicated  
to my parents

## ACKNOWLEDGEMENTS

I would like to thank my supervisor and advisor Dr. Kenneth S. Ball for his invaluable help in completing my research studies.

I would also like to thank Dr. Theodore L. Bergman for his helpful suggestions and for providing me with the initial outline of my research.

Furthermore, I would like to thank my co-reader Dr. Eric M. Taleff for all of his comments and suggestions which proved to be very helpful.

Dr. Myungho Song is thanked for all the times that he helped me getting over obstacles encountered at the beginning of my research work and for introducing me to a variety of oriental cuisines.

Mr. Gary A. Holtzman and Mr. Mark W. Silva are also thanked for a countless number of occasions where they alleviated my workload.

I would also extend my deep gratitude to Dr. Juan C. Morales for letting me take away a considerable amount of his time as he helped me out in many different ways. I as well want to thank Dr. Dah-Chyi Kuo for his help and advice.

I also thank Mr. Christopher W. Ramirez for his help in performing the experiments.

I would also like to thank Ms. Carol C.S. Hsu, Masahiko Matsumura, Mr. Francis H.R. França, and Mr. Chao-Ho "Charles" Lan for all the occasions when they helped me. Last but not least, I thank Dora C. Arévalo for all her patience and support.

Numerous other persons have helped me directly or indirectly in completing my tasks. I would like to thank them as well and I apologize for not mentioning them all by name.

Michael Gomon

# Experimental Study of Highly Viscous Impinging Jets

Michael Gomon, M.S.E.  
The University of Texas at Austin, 1997

Supervisor: Kenneth S. Ball

## ***Abstract***

The objective of this research is to study the behavior of highly viscous gravity-driven jets filling a container. Matters of interest are the formation of voids in the fluid pool during the filling process and the unstable behavior of the fluid in the landing region which manifests itself as an oscillating motion. The working fluids used in this research are intended to simulate the flow behavior of molten glass. Qualitative and

quantitative results are obtained in a parametric study. The fraction of voids present in the fluid pool after the filling of the container is measured for different parameter values of viscosity and mass flow rate. Likewise, frequencies of the oscillating jet are measured. Results are inconclusive with regard to a correlation between parameter settings and void fractions. As for frequencies, power law correlations are established.

## TABLE OF CONTENTS

List of Tables.....	vi
List of Figures .....	vii
Nomenclature .....	viii

### 1. INTRODUCTION

1.1 Introduction.....	1
1.2 Literature Review.....	2

### 2. EXPERIMENTS

2.1 Working Fluids.....	5
2.1.1 Introduction.....	5
2.1.2 Corn Syrup .....	5
2.1.3 Silicone Oil.....	6
2.2 Apparatus .....	6
2.2.1 Introduction.....	6
2.2.2 Corn Syrup Experiments .....	7
2.2.3 Silicone Oil Experiments.....	7
2.3 Measurements.....	7
2.3.1 Temperature .....	7
2.3.2 Weight.....	7
2.3.3 Void Fraction .....	8
2.3.4 Frequency.....	9
2.3.5 Velocity.....	9
2.3.6 Viscosity .....	11
2.4 Procedure.....	12
2.4.1 Introduction.....	12
2.4.2 Corn Syrup Experiments .....	12
(a) Viscosity Measurements .....	13
(b) Void Fraction Measurements .....	13
2.4.3 Silicone Oil Experiments.....	14

3. RESULTS AND DISCUSSION	
3.1 Corn Syrup Experiments .....	17
3.1.1 <i>Qualitative Results</i> .....	17
3.1.2 <i>Quantitative Results</i> .....	17
3.2 Silicone Oil Experiments .....	19
3.2.1 <i>Qualitative Results</i> .....	19
3.2.2 <i>Quantitative Results</i> .....	19
3.3 Comparison to Numerical Results.....	20
3.4 Comparison to Cruickshank and Munson (1981) .....	21
4. CONCLUSIONS AND RECOMMENDATIONS	
4.1 Conclusions .....	31
4.2 Recommendations .....	31
4.2.1 <i>Trial and Error</i> .....	31
4.2.2 <i>Future Work</i> .....	33
REFERENCES.....	34



## LIST OF TABLES

<b>Table 3.1:</b> Results of Small Fall Heights Experiments .....	22
-------------------------------------------------------------------	----

## LIST OF FIGURES

<b>Figure 2.1:</b> Comparing Viscosities vs. Temperature for the Working Fluid and Molten Glass .	15
<b>Figure 2.2:</b> Schematic of Experimental Apparatus .....	15
<b>Figure 2.3:</b> Schematic of Vertical Set-Up.....	16
<b>Figure 3.1:</b> Jet at Different Stages Upon Impact.....	23
<b>Figure 3.2:</b> Jet Pile-Up at a Later Stage .....	23
<b>Figure 3.3:</b> Flow Behavior of Analogous Fluid at Different Viscosities.....	24
<b>Figure 3.4:</b> Schematic of Experimental Apparatus .....	24
<b>Figure 3.5:</b> Results for Void Fraction Measurements for 42/43 Corn Syrup .....	25
<b>Figure 3.6:</b> Results for Void Fraction Measurements for 42/43 Corn Syrup .....	26
<b>Figure 3.7:</b> Results of Frequency Measurements for 60,000 cSt Silicone Oil.....	27
<b>Figure 3.8:</b> Results of Frequency Measurements for 60,000 cSt Silicone Oil.....	28
<b>Figure 3.9:</b> Results of Velocity Measurements for 60,000 cSt Silicone Oil.....	29
<b>Figure 3.10:</b> Sequence of Six Consecutive Frames Showing One Period of Jet Oscillation.....	30

## NOMENCLATURE

A	area, $m^2$
d	diameter, m
$F_d$	drag force, N
$f_v$	void fraction
g	gravitational acceleration, $m/s^2$
H	fall height, m
m	mass, kg
$\dot{m}$	mass flow rate, kg/s
Re	Reynolds number
r	radius, m
T	temperature, $^{\circ}C$ or K
V	volume, $m^3$
v	velocity, m/s

### Greek Symbols

$\mu$	dynamic viscosity, P (poise) or kg/m/s
$\nu$	kinematic viscosity, St (stokes) or $m^2/s$
$\rho$	density, $kg/m^3$

### Subscripts

air	referring to properties of air
c	receiving container
ldf	less dense fluid
wf	referring to properties of working fluid
s	sphere

## 1. INTRODUCTION

The United States Department of Energy (DOE) is considering several options for the immobilization of surplus weapons-grade plutonium. One of these is the "can-in-canister" option in which the plutonium is mixed with a solution of silicon oxide and metal oxides (National Academy of Science, 1994). It is then stored in small steel cans (approximately 7.5 cm in diameter by 40 cm in length). These cans are subsequently suspended on a rack, which is placed in a large stainless steel canister (71 cm in diameter by 305 cm in length). Finally, the canister is filled with molten glass, itself enriched with high-level nuclear waste. The filling process lasts about 24 hours as a thin stream of molten glass falls continuously into the canister. The main purpose for this vitrification process is twofold: first, the long-term secure storage of the nuclear waste in underground facilities has to be guaranteed not to cause any harm to the environment. Second, the issue of non-proliferation has to be resolved. The vitrification ensures that the nuclear waste will not leak into the environment for at least 30,000 years (long after the canister has disintegrated). The glass casting, containing a high level of nuclear waste, renders any attempt to recover the plutonium from the cans life-threatening and too difficult to be achieved within any tolerable time frame.

This "can-in-canister" option is only one of many plutonium disposition options being considered by the Amarillo National Resource Center for Plutonium (ANRCP). Other disposition options include the "deep borehole" option, in which the plutonium is buried in a very deep hole, and the "energy production" option, in which the plutonium is used in a reactor to generate useful electricity. The purpose of the ANRCP is to advance the science and technology, advise decision makers and inform the public on issues of concern to the Texas Panhandle region, the

state of Texas, and the U.S. Department of Energy in the use and disposition of materials from nuclear weapon disassembly (ANRCP, 1996). This purpose is accomplished through a variety of tasks, such as developing a state-of-the-art Electronic Resource Library to archive information on nuclear weapons material; conducting environmental studies in areas including groundwater treatability, bioremediation, risk assessment, atmospheric pollution, and pathway analysis; communicating with the public through informational videos, public service announcements, technical brochures, and other means; educating the public through a student research conference, a graduate assistantship, research and technology laboratories, a K-16 education project, and a variety of other methods; and performing studies of nuclear weapon materials storage issues, such as robotics, air surveillance, pit encapsulation, storage containers and aerosol dispersal.

The "can-in-canister" research conducted at The University of Texas at Austin is subdivided into four smaller projects to cover all thermal and fluid dynamics aspects of the filling process. In the first project, a small furnace is used to melt surrogate glass to perform small-scale experiments of the actual "can-in-canister" glass pour. Two other projects involve computer modeling of the glass pour. One simulates all aspects of the "can-in-canister" option while the other one concentrates on jet impinging characteristics, as outlined below. In cooperation with the latter project, low-temperature experiments with analogous fluids are conducted. These fluids have similar flow characteristics compared to molten glass and they can be used in experiments conducted at or close to room temperature. These low-temperature experiments constitute the fourth project and the subject-matter of this work.

Initial observations show that the flow behavior of the analogous fluids used in the low-temperature experiments matches that of molten glass in many aspects. It is noticed that the filling process of the canister is rather complex. Upon first impact onto the bottom of the canister, the fluid buckles and takes a spiraling motion. This is contrary to fluids with lower viscosities (e.g. water) which would exhibit a stable stagnation flow and spread out evenly. More specifically, several criteria have to be met in order for a fluid to buckle (Cruickshank & Munson, 1981). For once, a critical fall height has to be surpassed by the fluid. Also, the flow's Reynolds number based on outlet conditions of the jet (exiting a nozzle or orifice) has to be below a certain value, which depends on the shape of the jet (i.e. planar or axisymmetric). Due to the spiraling motion, the fluid develops a columnar pile-up. Eventually, the pile becomes unstable and slumps to one side. The fluid, continuing to spiral, builds up a new pile and the process repeats. As the filling process progresses, voids appear in the pool of fluid. Voids were also found to be present after previously conducted test fillings of a container with molten glass (termed "frit 165") at the Savannah River Site's (SRS) Defense Waste Processing Facility (DWPF). The appearance of these voids is of major interest in the current research since their presence is highly undesirable. Not only can they jeopardize the safety of the glass cast with regard to the environment but also the issue of non-proliferation is compromised due to possible crack formations in the glass cast. Furthermore, there is an economic issue at hand since the filling of one container is estimated to cost \$ 1 million. Therefore, the presence of voids, which essentially reduces the volume of discarded waste material per canister, increases the number of canisters that have to be filled which can lead to a significant surcharge considering that thousands of these canisters will be filled.

It is believed that voids are introduced into the pool due to the behavior of the fluid in the landing region as described above. The qualitative and quantitative study of the flow behavior in the landing region and, as a corollary, the voids and their formation are the main focus of the low-temperature experiments.

The motivation for performing low-temperature experiments is derived from the difficulties associated with molten glass as an experimental fluid. Besides the obvious qualifying factors in terms of flow behavior, experiments performed with an analogous fluid have to fulfill certain requirements in order to be regarded as feasible compared to pours with molten glass. The cost associated with those experiments should be significantly lower and the experimental procedure safer. Another aspect of performing low-temperature experiments lies in the fact that the effects of thermal radiation, by far the dominant heat transfer mode in the actual glass pour, can be isolated and other effects can be studied more closely.

## 1.1 LITERATURE REVIEW

Previous studies on highly viscous fluid flow have been performed notably by Taylor (1969), Buckmaster (1972), and Cruickshank and Munson (1981). Some related investigations include works by Zak (1985), Bejan (1987), Cruickshank (1987), and Tchavdarov, Yarin, and Radev (1993). In general, these reports are concerned with the onset of instability in the flow of highly viscous fluids as well as the nature of the instability. Taylor (1969) links the phenomenon of jet buckling for thin gravity-driven jets to an Euler instability, that is, he compares the buckling of the jets to the buckling of thin beams as studied in solid mechanics. He observes the behavior of glycerin and other fluids, including sucrose acetate isoburate and Tellus oil, in a variety of experiments, such as allowing the fluid to fall

through air or another less dense fluid, pulling the fluid by electric forces, or observing threads of the fluid whose ends are pushed or pulled. Taylor's results are mainly qualitative in nature, derived from photographs.

Although Taylor notes the tendency of viscous fluids to spiral, no attempt was made to quantify the frequency of the oscillations. Nothing was mentioned about formation of voids. Buckmaster (1972) performs a theoretical analysis of the problem and distances himself from Taylor's results by arguing that the buckling is induced by shear stresses instead of Euler instability. His analysis is based on fluids falling through liquids of almost equal density, thus being in a state close to neutral buoyancy. His analysis does not consider fluids falling through air or impinging onto a surface. Cruickshank and Munson (1981) deduce experimentally the critical height at which the flow becomes unstable (i.e. starts to buckle), using an apparatus where the fluid drops vertically onto a plate. The primary fluid they use in the experiments is silicone oil. Another fluid briefly examined is corn syrup. Two critical criteria for unstable behavior, both of which have to be fulfilled simultaneously, are established. First, either for a plane or an axisymmetric jet, values are determined for Reynolds numbers below which a fluid is guaranteed (given the second condition is met) to exhibit unstable behavior upon impact. Second, they state that a certain ratio of drop height over nozzle exit diameter is also necessary for buckling to occur. They as well describe that the initial buckling is planar folding which then develops into a spiraling motion. Additionally, they generate data that show the oscillation frequency for different flow parameters. The formation of voids (or "bubbles") is observed as the fluid is poured onto a pool of the same fluid. However, the void formation is regarded as undesirable for the conduction of the experiments and is avoided when possible. Cruickshank and

Munson's publication is the only one found by the author that allows for comparison with some of the results obtained in the experiments described in this work. Zak (1984) investigates the instability problem analytically and establishes criteria to determine the onset of instability. He bases his results on the thoughts established by Taylor and Cruickshank, adding that viscous fluids have features in common with elastic membranes and threads.

Bejan (1987) studies the buckling behavior of viscous fluids at low and high Reynolds numbers, giving a review of work done on the subject. He suggests linking a large number of buckling phenomena under common parameters of sinusoidal shape and a relationship between wavelength and transverse length scale. He acknowledges that the buckling inducing factors change with increase of Reynolds number but implies, in contrast to Cruickshank and Munson, that buckling occurs at high Reynolds number flows as well. Also, Bejan implicitly states that he sides with Buckmaster's view on viscous flow behavior in contrast to Taylor's Euler instability approach, which was also adopted by Cruickshank and Munson.

Cruickshank (1987) develops a theoretical model through a perturbation approach, breaking the flow into a near-wall and far-field region. He then compares his conclusions with his and Munson's experimental results from 1981 and finds good agreement. Cruickshank concedes that the only available experimental research with a quantified parametric study on the subject was the work he and Munson had done.

Tchavdarov et al. (1993) study the flow behavior analytically and numerically in a quasi-one-dimensional approach and are able to predict quantitatively the folding frequency of the jet. Their approach is the most comprehensive, linking previously established explanations concerning viscous fluid flow behavior into one model and

comparing their results with those of Cruickshank and Munson.

No qualitative nor quantitative study was found in the literature dealing with void formation and void entrapment caused by viscous flow behavior. Also, no work was found on experimental studies of flows in the viscosity range discussed in this work. The largest viscosity of a working fluid studied is Cruickshank's and Munson's 10,000 cSt silicone oil. The author's viscosity range for

the working fluids starts at 12,500 cSt and goes up to 200,000 cSt.

The objective of the low-temperature experiments is to study the instabilities associated with viscous flow behavior, as well as the void formation mechanisms and relationships between the flow parameters and the extent of void formation. A description of the experimental research is given and results regarding flow behavior in the landing region for different viscosities and void formation mechanisms are discussed.

## 2. EXPERIMENTS

### 2.1 WORKING FLUIDS

#### 2.1.1 Introduction

Before considering the overall experimental setup it is necessary to find a working fluid which exhibits flow properties such as density, surface tension, and viscosity, that are comparable to molten glass. For viscosity in particular, a wide range of values has to be matched to simulate molten glass as it falls through the canister. Preliminary test runs revealed that the temperature change the glass experiences as it travels from the nozzle exit downward to the bottom of the canister is quite significant. Estimates are in the range of up to 1 °C per cm of free fall (Plodinec, 1987). For the given height of the canister, this implies that the glass can undergo a temperature change of up to 400 °C, in which case the viscosity increases by more than three orders of magnitude from  $6.6 \times 10^3$  to  $8.5 \times 10^6$  cSt (Jerrell & Hardy, 1995). As a reference, water has a viscosity of approximately 1 cSt.

Molten glass above the glass transition temperature is treated as a Newtonian fluid (Viskanta, 1994). Since the flow phenomena which are to be investigated occur above the transition temperature, the analogous fluid used to simulate molten glass should also exhibit Newtonian flow characteristics. Furthermore, the fluid should be of reasonable cost and readily available on the market and not cause any health threat to the user. Finally, it should allow for flow visualization. This is necessary to study more closely the process of void entrapment, how voids are distributed in the pool, and what their sizes are. This implies the use of a transparent fluid, at least a fluid that can be made transparent through different methods (through filters, or infrared light).

Two suitable types of fluid meeting the above requirements were identified. The first fluid is 42/43 dextrose equivalent with a solid content of 80.3 % by weight, also known as 42/43 corn syrup. This corn syrup is commonly used in the food industry as a sweetener. The other fluid chosen is silicone oil, the principal fluid of choice for high viscosity flow experiments.

#### 2.1.2 Corn Syrup

Of all the common laboratory fluids that were considered for use, corn syrup proved to be the most suitable. It fulfills virtually all the requirements set forth for an analogous fluid. It is a translucent Newtonian fluid (Suleiman & Munson, 1981), does not cause a health threat to the user, and is readily available and inexpensive. As can be seen in Figure 2.1, the viscosity-temperature dependence is very strong. This enables the user to simulate the wide viscosity range of molten glass. Necessary thermophysical properties have been collected mainly from a publication by Chu and Hickox (1990). Figure 2.1 also shows the viscosity change with temperature for the molten glass as used in the DWPF test runs, termed "frit 165" (Soper & Bickford, 1982), over a range of 400 °C (650 to 1050 °C) as reported by Soper and Bickford (1982). This is the maximum temperature range the falling molten glass stream will encounter. The same viscosity values can be obtained with corn syrup over a temperature range of only 45 °C, a tenth of the range for molten glass. In addition, this range (-2 to 42 °C) is more readily controlled in a laboratory environment. Another good fit is density, which is of the same order (approximately  $1420 \text{ kg/m}^3$  for corn syrup compared to approximately  $2400 \text{ kg/m}^3$  for molten glass). One drawback encountered is the comparably low surface tension of the syrup (approximately 0.068 N/m), which is orders of magnitude lower than the range of values for molten glass.



### 2.1.3 *Silicone Oil*

The primary difference between corn syrup and silicone oil for the purpose of this work is that silicone oil has a viscosity that is fairly insensitive to temperature. Standard viscosities are provided in a wide range (from 0.65 to 100,000 cSt and larger) by the manufacturer (Dow Corning of Midland, Michigan). Silicone oil, like corn syrup, is a Newtonian fluid (Suleiman & Munson, 1981). There are a few aspects that have to be taken into consideration when using silicone oil compared to corn syrup. A major benefit of using silicone oil is that the temperature control that is necessary when using corn syrup is not needed with silicone oil. On the other hand, its insensitivity makes it necessary to replace it in the experimental apparatus whenever a different viscosity is desired. Also, its surface tension is only one third that of corn syrup, which sets it even further apart from molten glass, as does its density ( $975 \text{ kg/m}^3$ ).

Another property of silicone oil is found to be a major inconvenience as well. In particular at higher viscosities (larger than 1,000 cSt), the solubility of silicone oil in liquids that are used as solvents at lower viscosities is very small or non-existent. Whereas corn syrup can be removed from practically any surface by diluting it with hot water, only mechanical ways were found to be effective in the removal of silicone oil from surfaces to be cleaned, requiring considerable effort. The higher cost of silicone oil prevented its usage to the same extent as corn syrup (silicone is almost ten times as expensive as corn syrup, which sells for under \$ 15 per 20 liters).

## 2.2 APPARATUS

### 2.2.1 *Introduction*

One of the intrinsic problems encountered with the study of highly viscous fluids is that of transporting the fluid through

pipes and nozzles and ensuring a consistent flow rate. The majority of commercially available pumps is not capable of moving fluids that have the viscosity range encountered in this research. Therefore, instead of a pump, a hydraulic cylinder is used since the driving force for a piston-cylinder arrangement is for the most part only restricted by the size of the motor used to push the piston. A schematic of the experimental setup can be seen in Figure 2.2. The apparatus is positioned on top of two by two stacked laboratory desks, providing a height of 2 m, which is close to the midpoint falling height for the molten glass. The apparatus itself consists of the following components: (a) a motor with 1/2 hp output, a speed reducer, and a variable input controller; (b) a traversing mechanism consisting of a threaded rod and a frame, where the frame is pushing a piston inside a hydraulic cylinder, and (c) the hydraulic cylinder, which is 7.6 cm in diameter and holds a volume of up to 3.8 liters of the analogous fluid. A nozzle system is attached to the front of the cylinder, allowing the fluid to be directed downward. Figure 2.3 shows the vertical setup. After exiting the nozzle, the fluid falls under the influence of gravity through a vertical arrangement consisting of two concentric pipes: a metal inner pipe and an outer PVC pipe. The fluid then drops into a rectangular receiving container made of acrylic (bottom made of a 3.2 mm thick copper plate). The acrylic is 1.27 cm thick; the inside measures 15.25 cm by 15.25 cm with a height of 25.4 cm. An electronic laboratory scale at the bottom of the vertical setup, on which the receiving container is placed, is used to monitor the weight of the receiving container as it is filled with the working fluid.

### 2.2.2 *Corn Syrup Experiments*

For experiments that use corn syrup as the working fluid, additional environmental control has to be imposed on the basic

experimental setup to hold the syrup at a particular desired temperature (and thus viscosity) level.

The following steps are taken to control the thermal environment of the experimental apparatus. First, the piston as well as the cylinder are wrapped with Tygon tubing which is connected to constant temperature baths and which itself is insulated with pipe insulation. The piston, cylinder, and nozzle system are also encased in insulation material. Tygon tubing is also wrapped between the inner and outer pipe of the vertical setup and connected to a constant temperature bath. Additionally, the outer pipe is insulated. The assembly below the vertical pipes is also encased in insulating material. A heat exchanger is placed above the electronic scale and is in contact with the copper bottom of the receiving container. The heat exchanger is connected to a constant temperature bath. A total of four temperature baths are incorporated in the temperature control setup. In order to monitor the temperature at different stages of the apparatus, thermocouples are placed as follows: one thermocouple is placed each at the rear, middle, and front part of the hydraulic cylinder; one thermocouple is placed at the nozzle, which is made of brass; another one is placed at the bottom of the vertical pipe. A thermocouple is also placed inside the heat exchanger.

### **2.2.3 Silicone Oil Experiments**

As mentioned in Section 2.2.1, silicone oils, whose nominal viscosities are specified for room temperature (25 °C), do not need environmental control to maintain their viscosity value. Therefore, none of the additions to the basic experimental apparatus to ensure an acceptable environmental control for corn syrup have to be employed for silicone oil.

## **2.3 MEASUREMENTS**

### **2.3.1 Temperature**

Temperature measurements are only required when using corn syrup as the working fluid, since its thermophysical properties are strongly dependent on temperature. Six type K thermocouples (manufactured by Omega Engineering, Inc., of Stamford, Connecticut) are placed along the experimental apparatus as described in Section 2.2.2. The temperatures are kept steady by employing four temperature baths which circulate a mixture of water and ethylene glycol through the tubes around the cylinder and the vertical setup and through the heat exchanger at the bottom of the vertical setup. The temperature baths are one Haake A82, manufactured by Haake GmbH of Karlsruhe, Germany, and three Isotemp 1030P, manufactured by Fisher Scientific of Pittsburgh, Pennsylvania. All temperature baths have a volume capacity of approximately 10 liters and a temperature range between -30 to +120 °C. The thermocouples are connected via a signal conditioning system to a data acquisition board and monitored by use of a commercial data acquisition software (LabVIEW 4.0), all of which are manufactured by National Instruments Corporation of Austin, Texas. The uncertainty in the thermocouples measurements is estimated to be plus or minus 0.5°C.

### **2.3.2 Weight**

An electronic laboratory scale is put to use to measure weight. The scale is manufactured by Sartorius AG of Göttingen, Germany (Model QC 34EDE-S) and has a capacity of up to 34 kg with a resolution of 0.5 grams. The base of the scale has dimensions of 30 cm by 40 cm. The manufacturer's accuracy and precision for the single load-cell scale are provided as  $\pm 1$  gram, which was experimentally verified. For mass

flow rate measurements, a stop watch is attached next to the scale's display and the read-out of both the scale and the stop watch are recorded with a color VHS video camera (Palmcorder IQ VM565 manufactured by Quasar of Secaucus, New Jersey) placed on a tripod. The video camera has a 14X built-in optical zoom and can record for up to 30 minutes using VHS Compact tapes. The uncertainty in the measurements is estimated by dividing the entire filling process into intermediate intervals (taken from the VHS tape) and analyzing the results in a statistical manner (Student's t-distribution), as outlined in Beckwith and Marangoni (1990). The uncertainty of the stop watch measurements is neglected; the manufacturer (Casio Computer Co., Ltd., Tokyo, Japan) claims an accuracy of plus or minus ten seconds per month. The stop watch is not used for more than thirty minutes in any one experiment. For thirty minutes, the uncertainty is less than 0.007 seconds, which is less than the resolution of the watch (0.01 seconds). As with all uncertainties calculated in this research, the confidence level is chosen to be 95%.

### **2.3.3 Void Fraction**

The technique used to determine the void fraction is based on Archimedes's principle (Tipler, 1991). The receiving container together with the fluid inside is submerged into another fluid of lesser density and held suspended with a string attached to a horizontal hook. The two fluids are insoluble with each other over the duration of the measurement. The difference in weight before and after submerging the container can be used to determine the volume of the container with the working fluid inside, since it is equal to the displaced volume of the less dense fluid, whose density is known. To obtain the volume of the working fluid, the volume of the container alone, which was previously determined from experiments with a submerged empty container (including the

string attached to it), is simply subtracted. Knowing the mass of the working fluid in air from the scale allows calculation of the volume of the working fluid as if it has no voids. Knowing the volume of the working fluid with the voids entrapped and the volume with no voids entrapped can then be used to determine the fraction of voids in the fluid.

A few notes should be added for clarification: Voids do escape during the measurements. To account for this and to be able to extrapolate the void fraction that is present immediately after the end of the pour, the temporal change of the weight of the container with the syrup inside is continuously monitored starting from the end of the pour (when the container with the fluid is submerged into the bucket) and continuing for up to 30 minutes. This allows the weight loss due to escaping voids to be determined as a function of time, so that the weight right after the end of the pour can be determined. Consequently, the void fraction present immediately after the pour can be estimated. This procedure also takes into account different rates of weight loss due to different temperature gradients between the working fluid and the less dense fluid since different curves are generated for different temperature gradients. For either of the working fluids chosen, changes in density due to temperature changes during the void fraction measurements are negligible (at the most 0.56% for corn syrup and 0% for silicone oil).

Voids also escape from the pool during the pour. However, the assumption made is that in the actual molten glass filling process voids will also escape through the pool and will not contribute to the overall void fraction after the pour. Therefore, the void fraction calculation does not take into account the voids that escaped during the pour. This also implies that all of the void fractions measured are conservative estimates. The following shows the calculation of the void fraction reduced to masses being

measured and the ratio of the densities of the submerged and submerging fluids. As can be seen from the equation, the only uncertainties

are in the scale measurements and the density values.

$$f_v = \frac{m_{ldf} - m_c - \frac{\rho_{ldf}}{\rho_{wf}} m_{wf}}{m_{ldf} - m_c} \quad (1)$$

where

$f_v$  = void fraction (by volume)

$m$  = mass

$\rho$  = density

and the subscripts are:

$c$  = receiving container (empty, suspended in lower density fluid)

$ldf$  = less dense fluid

$wf$  = working fluid

With a few exceptions to confirm repeatability of the experiments, most parametric configurations in the experiments occur only once. Therefore, a single-sample uncertainty analysis is adopted to estimate the error in the results. The standard reference for this kind of uncertainty analysis is Kline and McClintock (1953).

### 2.3.4 Frequency

During the pour, with the aid of a high speed camera, the oscillations of the jet in the landing region are recorded for different flow parameters and later analyzed on a frame-by-frame basis. The camera used is a Motionscope HR2000 manufactured by Redlake Camera Corporation of San Diego, California. The key specifications of the camera are: monochrome; up to 2,000 frames per second recording with a maximum storage of 8 seconds (longer for lower frame rates); variable play back rates from 1 to 4,000 frames per second; electronic shutter up to 1/40,000 s; 160x140 pixel resolution for 2,000 frames per second (higher for lower frame rates). The camera recording is dubbed onto a VHS tape with a play back rate of 1 frame per second, which allows the frequency of jet spiraling to be determined manually.

The accuracy of the frequency measurement varies with the number of frames per revolution. For each measurement the number of frames for 5 revolutions is taken as the basis for one frequency measurement. At least 10 measurements are made in this manner for each experiment and the uncertainty for each measurement is (conservatively) estimated to be within 2 frames. The uncertainties are then calculated with Student's t-distribution (Beckwith & Marangoni, 1990) under the assumption that the data distribution is symmetric about the mean value.

### 2.3.5 Velocity

For the velocity measurements, food coloring is injected into the stream and a scale is placed inside the receiving container next to the falling jet, allowing the drops of food coloring to be tracked as they pass the scale. The high speed camera again makes it possible to analyze footage and to determine the velocity of the drops. For this, the number of frames needed for a drop to travel a certain distance (taken from the scale) is determined and then converted into velocity. The uncertainty is estimated to lie within one frame for the distance fallen. Several

measurements are taken for each flow rate to establish the basis for a statistical estimate of the error, again employing Student's t-distribution due to the small number of

samples. The results for velocity are compared to the Torricelli limit, which computes the velocity of a free-falling body from a given height with no initial velocity:

$$v = \sqrt{2gH} \quad (2)$$

where

$g$  = gravitational acceleration

$H$  = fall height

$v$  = velocity

From the velocity and the mass flow rate measurements the diameter of the jet in the landing region can be determined:

$$\dot{m} = \rho v A \quad (3)$$

where

$A$  = cross-sectional area

$\dot{m}$  = mass flow rate

$\rho$  = density

$v$  = jet velocity in landing region

The cross-sectional area of the jet is:

$$A = \frac{\pi}{4} d^2 \quad (4)$$

where

$d$  = jet diameter

Combining equations (3) and (4) and solving for  $d$ :

$$d = \sqrt{\frac{4\dot{m}}{\pi\rho v}} \quad (5)$$

In addition, knowing the diameter and the mass flow rate allows to determine the local Reynolds number in the landing region:

$$Re = \frac{vd}{\nu} \quad (6)$$

where

$Re$  = Reynolds number

$\nu$  = kinematic viscosity

Equation (6) can be combined with equations (3) and (4) to yield:

$$Re = \frac{4\dot{m}}{\pi\nu d} \quad (7)$$

### 2.3.6 Viscosity

For low Reynolds numbers ( $\ll 1$ ), the drag force experienced by a sphere can be approximated by (Fox & McDonald, 1992):

$$F_d = 6\pi\mu v_s r \quad (8)$$

where

$F_d$  = drag force  
 $\mu$  = dynamic viscosity  
 $v_s$  = velocity of sphere  
 $r$  = radius of sphere

Assuming a drop of air rising in a pool of (viscous) working fluid, a force balance yields that the gravitational force and the drag

force are opposed by the buoyancy force (when the droplet has reached terminal velocity):

$$\rho_{\text{air}} V_{\text{air}} g + 6\pi\mu v r = \rho_{\text{wf}} V_{\text{wf}} g \quad (9)$$

where

$\rho$  = density  
 $V$  = volume  
 $g$  = gravitational acceleration  
subscripts:  
air = air droplet  
wf = working fluid

Noting that the volumes of the air and the working fluid are the same (since the air displaces its own volume in the working

fluid), and assuming the shape of the drop to be spherical, the volume  $V$  can be expressed as:

$$V = \frac{4}{3} \pi r^3 \quad (10)$$

Replacing  $V$  in Equation (4) with (5) and solving for the viscosity:

$$\mu_{\text{wf}} = \frac{2}{9} \frac{r^2 g}{v_s} (\rho_{\text{wf}} - \rho_{\text{air}}) \quad (11)$$

where the density of air is negligible compared to the density of the working fluids used in this work:

$$v_{\text{wf}} = \frac{2}{9} \frac{r^2 g}{v_s} \quad (12)$$

where

$v$  = kinematic viscosity

Note that equally sized air bubbles will rise slower in fluids with larger viscosity. Assuming a spherical form of the air droplet in a viscous fluid, the only measurements that need to be taken are the diameter and the velocity of the rising air bubble.

Uncertainties arise from these measurements, where the effective radius measurement error is squared. A number of experiments are performed for each viscosity measured so that a statistical approach can be utilized to approximate the uncertainties involved.

## 2.4 PROCEDURE

### 2.4.1 Introduction

The experimental procedures for the two different working fluids are quite distinct. One reason lies in the previously mentioned fact that the use of silicone oil, in contrast to corn syrup, does not require temperature control to maintain the thermophysical properties. The other reason is that not all of the equipment mentioned in the previous section was available from the start of the experiments. Therefore, no frequency or velocity measurements were performed with corn syrup, the first working fluid. On the other hand, as will be explained in section 4.2.1, some of the properties of silicone oil render it infeasible to perform any void fraction measurements. Also, the manufacturer provided the standard viscosities so that no viscosity measurements are necessary. Therefore, the experiments performed with corn syrup and silicone oil turn out to be exclusive from one another, i.e. no experiment is the same for both working fluids. The only direct comparison of the two fluids lies in a qualitative analysis of the flow

$$\mu = 0.2412 \exp \left[ 12.5867 \exp \left( -\frac{T}{55.7805} \right) \right] \quad (13)$$

where

$T$  = temperature (in °C)

$\mu$  = dynamic viscosity (in poise)

behavior in the landing region. The following sub-sections describe the experimental procedures that are performed for each of the working fluids.

### 2.4.2 Corn Syrup Experiments

#### (a) Viscosity Measurements

For the viscosity measurements, a sealed acrylic container filled with corn syrup is immersed into a water bath (a larger acrylic container filled with water) whose temperature is controlled immersed copper tubes connected to a constant temperature bath. Depending on the viscosity desired, the container has to be immersed in the bath for up to 36 hours for the syrup to reach thermal equilibrium. Once in equilibrium, a syringe filled with air is lowered into the syrup and air bubbles are injected into the fluid. During the duration of the experiment, the container filled with syrup stays in the water bath which is continuously held at the desired temperature. A scale is placed inside the syrup container to measure the diameters of the air bubbles. A VHS (compact) video camera records at a large zoom (up to 14X) the rising of the bubbles as they pass the scale. To minimize measurement errors, the depth of field for the camera is kept small so that only bubbles close to the ruler stay in focus. At least seven air bubbles are observed for each temperature setting. Then, equations (11) and (12) are used to calculate the dynamic and kinematic viscosity, respectively. The results are then compared to equations published by Chu and Hickox (1990) relating 42/43 corn syrup temperature to viscosity and density:

and

$$\rho = \frac{14,255,000}{1 - 74.5333 + 3.5691T + 0.0078788T^2} \quad (14)$$

where  $T$  = temperature (in °C)  
 $\rho$  = density (kg/m<sup>3</sup>)

Equations (8) and (9) can be combined to obtain a relationship between kinematic viscosity and temperature:

$$v = \frac{3,438,306 \exp \left[ 12.5867 \exp \left( -\frac{T}{55.7805} \right) \right]}{1 - 74.5333 + 3.5691T + 0.0078788T^2} \quad (15)$$

where  $v$  = kinematic viscosity (in m<sup>2</sup>/s)

#### (b) Void Fraction Measurements

Each experimental run can be subdivided into four major steps. First, the hydraulic cylinder has to be filled with the analogous fluid such that no air bubbles are present in the fluid before it is poured. Second, the initial environmental conditions have to be established. Third, the fluid is poured into the receiving container during which jet spiraling frequency measurements can be taken. Fourth, the void fraction is measured after the pour.

For step one, in order to make sure that the fluid inside the cylinder is free of air bubbles, any bubbles in the fluid reservoir have to be removed before the cylinder is loaded with fluid. Then, the cylinder must be filled in such a manner so that no air enters the cylinder. The filling process was modified several times until a satisfactory solution was found. A 19-liter (5-gallon) pail is placed in front of the cylinder and connected to the nozzle system. This setup is chosen since it is observed that the fluid, after being poured into the pail and standing for 48 hours, is completely devoid of air bubbles. The filling process is achieved by pulling the piston slowly back, thus drawing the fluid into the cylinder, a process that takes about 3 hours. Since approximately 4 liters are used

for one experimental run, four to five experiments can theoretically be performed consecutively before refilling the pail, after which another wait of two days is necessary to let air bubbles escape. To ensure that no air bubbles are present in the cylinder after it is refilled, any two consecutive runs are carried out with at least one full day (24 hours) between them to allow any remaining air bubbles in the fluid to escape.

For experiments that require the fluid to be different from room temperature, the constant temperature baths are turned on and set to the desired temperature. The temperature is then monitored at the different positions along the apparatus. Once the thermocouples indicate the set temperature has been reached, the cylinder is held at that state for an additional 30 hours to ensure that the fluid is at a uniform temperature. A one-dimensional heat transfer analysis for the highest possible temperature difference between the fluid and the environment, assuming energy transport by diffusion only, predicts 26 hours as the time to reach thermal equilibrium.

The next step is the pouring of the fluid. Right before the pouring, the temperature values are read and double-checked with a portable multimeter (Fluke



8840A, Fluke Corporation, Everett, Washington). If the temperatures are within the tolerance limit (1 °C), the experiment proceeds. In that case, the logging time for the data acquisition system is changed from 20 minutes to 1 second to monitor the temperatures during the pour.

A variable-speed control unit at the motor allows the flow rate to be varied. While starting the recording for the scale output, the nozzle valve and the control unit are operated simultaneously. The valve for the nozzle can be opened and closed remotely so that the environmental control is not compromised during the pour. The flow rate set by the control unit is only a nominal value; a more accurate assessment of the flow rate can be determined from the data taken by the electronic scale positioned below the receiving container.

Finally, quantitative measurements to obtain the void fraction in the container are performed after the pour. The method to determine the void fraction is based on Archimedes's principle, as outlined in the previous section. The container filled with analogous fluid is immersed and suspended in de-ionized and distilled water (which ensures a consistent value of density), contained in a large bucket. Below the bucket, an electronic laboratory scale monitors the weight.

### *2.4.3 Silicone Oil Experiments*

For the experiments using silicone oil, a high speed camera is placed in front of the receiving container to record the behavior of the working fluid in the landing region. In addition to the high speed camera, two strong light sources (250 watts each) have to be used to ensure proper lighting conditions. The frame rate of the camera is set to 2,000 frames per second and the shutter speed to 1/6,000 of a second. The pouring process is analogous to the one for corn syrup described in the previous section (except for the temperature control). For the frequency measurements, two sequential recordings are made per pour (the pour not being interrupted), filling the camera's storage capacity of 8 seconds or 16,000 frames. A number of experiments are conducted at the same mass flow rate (as permissible by the control unit setting) to check results for repeatability.

For the velocity measurements, food coloring droplets are traced with the high speed camera and the recording is made for 8 seconds without interruption. After the experimental runs, the recordings are transferred onto a regular VHS tape at a play back rate of one frame per second and analyzed.

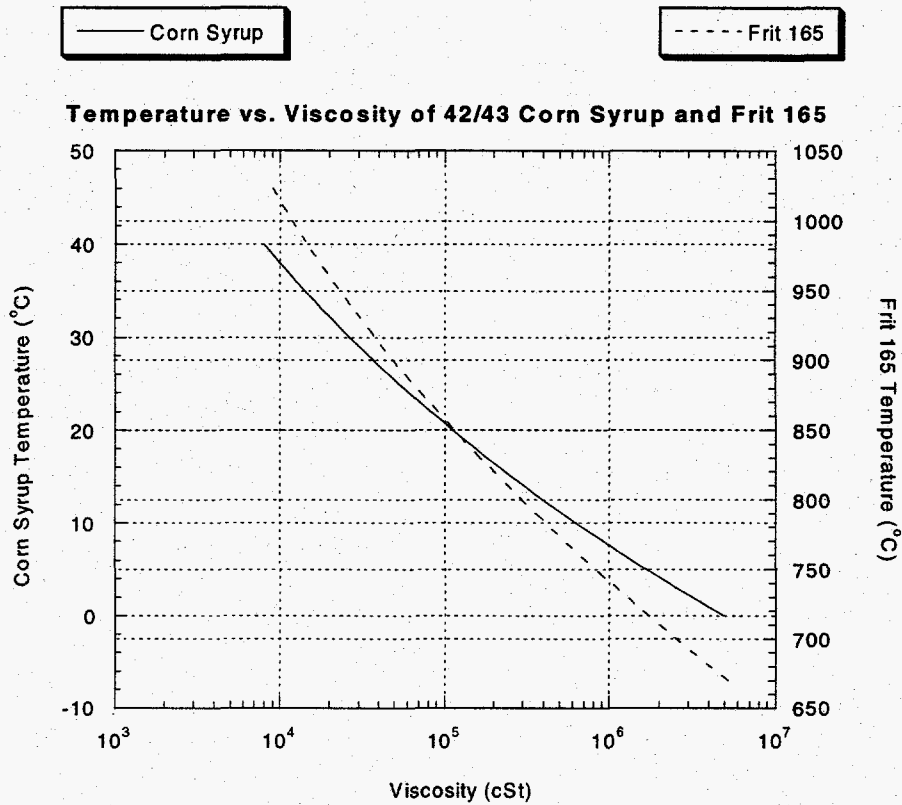


**Figure 2.1:** Comparing Viscosities vs. Temperature for the Working Fluid and Molten Glass

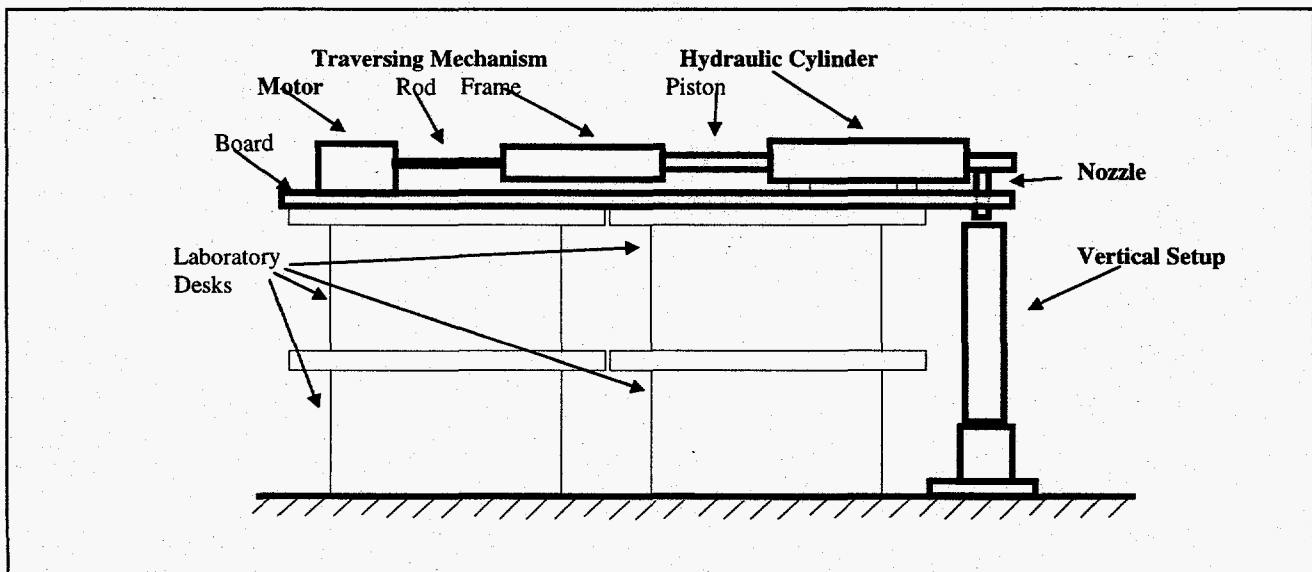


**Figure 2.2:** Schematic of Experimental Apparatus

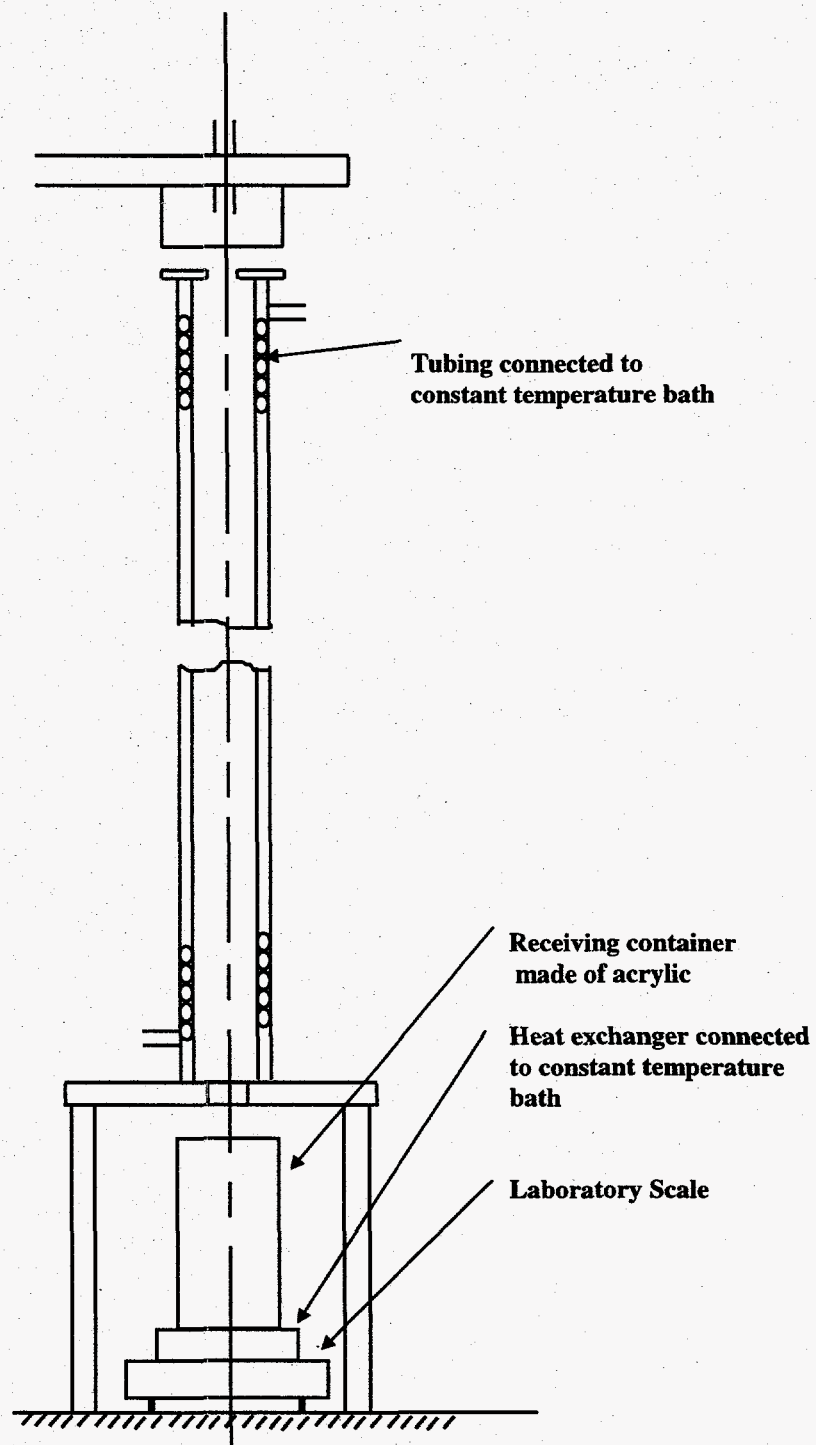


**Figure 2.3** Schematic of Vertical Set-Up

### 3. RESULTS AND DISCUSSION

#### 3.1 CORN SYRUP EXPERIMENTS

A series of pours is conducted to visually detect the instabilities of the impinging viscous jet and to determine characteristics of void entrapment. Also, a parametric study of void fractions is performed with pour rates and viscosities being the independent variables. The effective fall height for the fluid is 1.7 m for all experimental runs.

##### 3.1.1 Qualitative Results

A number of qualitative results is obtained by observing the flow behavior with different viscosities in the landing region. Figure 3.1 shows different stages of the jet upon impinging. The buckling of the jet immediately after impact and the thickening of the jet toward the bottom are clearly visible. The jet then starts to fold over and eventually exhibits a spiraling motion behavior. Figure 3.2 shows the jet at a later stage, still spiraling and forming a pile-up.

Figure 3.3 summarizes the flow behavior for three distinct investigated viscosities serving as examples for "low," "medium," and "high" viscosities as encountered in the experimental runs. The height of the fluid pile-up is found to be proportional to the magnitude of viscosity. Also, the spiraling amplitude is larger for higher viscosities. In addition, higher viscosity flow leads to increased slumping activity, i.e. instability of the jet pile-up. For a medium viscosity, the pile-up is smaller, as is the amplitude of the oscillations. The size of the voids is small compared to the high viscosity case. For the low viscosity, or high temperature experiment, it is found that the pile-up is very small, as is the amplitude of the spiraling. The voids are small in size compared to the other higher viscosity cases.

It is also found that the mass flow rate affects the nature of the slumping motion. At

lower mass flow rates (smaller diameters) the slumping occurs more often than at higher mass flow rates, on average. Mass flow rate also determines the frequency of the oscillations. The higher the mass flow rate, the smaller is the observed frequency.

In summary, the following qualitative conclusions can be drawn: the pile-up height, the amplitude, and the void size all are proportional to the magnitude of the viscosity. The frequency of the oscillating jet is inversely proportional to the mass flow rate as is the rate of slumping in the landing region.

The main void formation mechanism observed is believed to be the oscillatory pile-up/slumping motion of the pile. As the fluid coils up, air is trapped inside the pile column. When the pile becomes unstable and starts to slump over, the air is trapped and pushed into the pool of fluid. The air is then forced to the outer regions of the pool as more fluid enters the pool in the center region of the receiving container.

##### 3.1.2 Quantitative Results

For the scope of this work, the most important parameter for flow behavior of corn syrup is its viscosity. Due to the strong viscosity-temperature dependence the accurate determination of the viscosity for a given temperature is necessary.

Hence, one of the first experiments conducted has the purpose of verifying or replacing the temperature-viscosity relationships (Equations (13), (14), and (15)) of corn syrup found in the literature (Chu & Hickox, 1990). Several experimental runs are performed at five different temperatures as outlined in Section 2.3.6, covering the range of temperatures for the void fraction measurements. This is a summary of the results: the velocities of the air bubbles rising in the fluid range from  $3.0 \times 10^{-5}$  m/s to  $1.0 \times 10^{-3}$  m/s, mainly depending on viscosity. The radii measured range from  $2.0 \times 10^{-3}$  to  $4.0 \times 10^{-3}$  m. The mean value and a 95% confidence

interval are determined and plotted in comparison with the values obtained by utilizing the published equation for the corn syrup viscosity as a function of temperature (Chu & Hickox, 1990). The plot is shown in Figure 3.4 and it can be observed that the measured values are in good agreement with equation (13). Therefore, it is decided to use the established relation from the literature to determine viscosities at intermediate temperatures for which no measurements were performed.

There is an upper and lower limit found for the mass flow rate. The upper limit is coupled with the viscosity of the working fluid. The highest viscosity is limited by the temperature control capabilities (i.e. the effectiveness of the insulation). To be able to maintain an uncertainty in the temperature measurements of 1 °C, the lowest temperature is 16 °C. On the other hand, the highest temperature is 30 °C. With a temperature of 16 °C, the motor manages to obtain a maximum mass flow rate output of about 40 g/s, which hence is the upper limit. The lower limit for the mass flow rate is also established. Since the motor output is quite irregular for small values of rpm (revolutions per minute), the mass flow rates measured at these conditions have large standard deviations. The lower limit for a mass flow rate with a reasonable range of uncertainty is found to be 5 g/s. Hence, the parametric ranges for the experimental runs are established: the mass flow rate can be varied from 5 g/s to 40 g/s and the temperature can be varied from 16 °C to 30 °C. This temperature range results in a corresponding viscosity range from  $2.14 \times 10^5$  cSt to  $2.65 \times 10^4$  cSt, respectively. This is equivalent to molten glass ranging in temperature from 815 °C to 940 °C. Compared to the molten glass mass flow that has mass flow rates between 19 g/s to 25 g/s, the corn syrup mass flow rates cover a significantly larger range, which facilitate the investigation of the role of the mass flow rate

on the behavior of the jet in the landing region.

For the corn syrup experiments, 29 of the performed experiments yield acceptable data for void fractions in a parametric study of mass flow rate and viscosity. Experiments performed at a temperature of 16 °C had to be removed from consideration since they yielded unacceptably high uncertainty limits. The uncertainty for the void fraction measurements for all other experiments is found to be consistently within 0.17 percentage points regardless of viscosity and mass flow rate. For example, when a void fraction of 1% is measured, the uncertainty is about plus or minus 0.17%. If a void fraction of 5% is measured, the uncertainty is still plus or minus 0.17%. Figure 3.5 contains all data points collected, where the void fraction is shown versus the mass flow rate. Several statements can be made from this graph. First, the range of void fractions measured lies between about 1.7 to 4.5%. Second, for none of the nominal viscosities could a monotonic relationship between void fraction and mass flow rate be established. Third, with one exception no monotonic relationship between void fraction and viscosity could be established. The exception lies in the data points collected for the highest mass flow rate at about 38 g/s, as can be observed in Figure 3.5. From those, it is found that the void fraction increases with decrease in viscosity. Figure 3.6 shows the data points with the abscissa now representing viscosity. Also from this graph, no monotonic relationship between the variables is detectable. As mentioned in section 2.3.3, voids that escape during the pour are not accounted for. Since the pours take longer for lower mass flow rates, one might expect that in general the void fractions should be smaller for low mass flow rates and higher for high mass flow rates. However, even this trend cannot be established from the figures.

The Reynolds number based on outlet conditions ranges from 0.002 to 0.1, the local values in the landing region are between 0.02 to 0.54, based on the Torricelli limit (see Equation (2)). Hence, no case is run where the Reynolds number surpasses the maximum critical value of 1.2 for jet buckling of axisymmetric jets suggested by Cruickshank and Munson (1981). In all experiments the syrup is observed to be oscillating in the landing region. In none of the experiments is jet breakup detected. Due to the fact that a high speed camera was not available until after the working fluid was changed from corn syrup to silicone oil, no frequency measurements nor velocity measurements were performed with corn syrup as the working fluid.

### 3.2 SILICONE OIL EXPERIMENTS

Two different viscosity silicone oils are used in separate series of experiments. One has a standard viscosity of 60,000 cSt, the other a viscosity of 12,500 cSt. The frequency (for both fluids) and the velocity (for the 60,000 cSt fluid) are both measured as a function of mass flow rate. The effective fall height for most of the experiments is 1.7 m. See Section 3.3 (Comparison to Numerical Results) for exceptions.

#### 3.2.1 Qualitative Results

The overall behavior of silicone oil in the landing region is comparable to the behavior of corn syrup. However, some peculiarities of silicone oil which can be derived from its lower surface tension do set it apart from corn syrup. For example, air bubbles are located right on the top surface of the pool forming a covering layer. For corn syrup, air bubbles are more evenly distributed in the pool. Also, for some of the high mass flow rate experiments with the 12,500 cSt fluid, a different flow regime is observed, as discussed in the following section.

#### 3.2.2 Quantitative Results

The results for the frequency vs. mass flow rate experiments are analogous for a certain range of mass flow rates. It is found that for the 60,000 cSt fluid the relationship of frequency to mass flow rate can be expressed in form of a power law (Figure 3.7) over the entire range of mass flow rates used. The curve fit for the 16 data points shows that the power law correlation is captured by just about all uncertainty bars imposed on the data points. The results for the 12,500 cSt fluid (Figure 3.8) show a different picture. For the frequencies for mass flow rates up to about 14 g/s, a power law relation can be established. One data point in that regime had to be removed and at this point it is not clear why that point does not fit in the relation. At a mass flow rate of about 16 g/s, the spiraling motion of the fluid in the landing region is no longer prevalent. Instead, a planar folding sets in so that spiraling and planar folding exchange. This behavior contributes to the difficulty of adding data points to the graph since oscillating and folding yield different frequencies and obviously are the reason why the power law fit is no longer valid for mass flow rates higher than about 15 g/s. For a mass flow higher than about 19 g/s, planar folding becomes the only mode of motion as spiraling is in effect no longer observed. For mass flow rates in excess of about 23 g/s, neither oscillations nor planar folding are detectable. At no point during the experiments is jet breakup detected.

For the velocity measurements (60,000 cSt), no particular trend can be established for changes in mass flow rate. Six different mass flow rates yield velocities that average to 4.8 m/s (Figure 3.9). The uncertainty is fairly large (close to 10%). However, even the highest velocity in the confidence intervals still does not approach the Torricelli limit of about 5.7 m/s. Thus, it can be deduced that viscous drag is a factor in the velocity development. Also, due to the

fact that the velocity shows no particular trend compared to mass flow rate, the only way to conserve mass flow is for the diameter to become larger with increase in mass flow rate. Also, the velocity contribution of the cylinder pushing the fluid through the nozzle is found to be negligible, since for the highest possible flow rate the velocity at the outlet only contributes about 6% to the velocity in the landing region, an amount which is within the uncertainty limits for the velocity measurements in the landing region. Local Reynolds numbers in the landing region range from 0.43 to 1.4 for the 12,500 cSt fluid and from 0.09 to 0.28 for the 60,000 cSt fluid (based on the Torricelli limit). Using equation (5), the diameter in the landing region is found to be from 1.2 mm to 2.9 mm (based on the average value of 4.8 m/s).

Regarding the direction of flow during oscillatory motion, out of 35 recorded directions, 20 are found to be clockwise and the remaining 15 counterclockwise. The frequency itself does not seem to have any effect on the preferred direction of spiraling. Also, no preference can be attributed to mass flow rates. In several cases, again with no parametric dependency detectable, the flow direction changed from clockwise to counterclockwise after the pile-up slumped over to one side and a new column formed. Hence, no preferred direction of spiraling is detected.

The diameter close to a fall height of 1.7 m can be considered fully developed (at least with regard to the experimental results and their uncertainties). In none of the frequency experiments is a trend observed of either increase or decrease in frequency when footage which shows different pool heights from the same run are analyzed.

### 3.3 COMPARISON TO NUMERICAL RESULTS

A series of experiments is also performed to enable a direct comparison

between experiments and numerical results. The numerical results are achieved by the commercial Computational Fluid Dynamics (CFD) code Flow-3D (Flow Science, Los Alamos, New Mexico) and are reported separately by Silva (1997). A total of six experimental runs are performed, two for the 60,000 cSt silicone oil and four for the 12,500 cSt oil. In order to match the computational domain in the numerical simulations, the effective fall height has to be reduced considerably from 1.7 m to less than 0.4 m. Since the diameter of the jet is now in the developing range the frequency is highly dependent on the instantaneous fall height. Table 3.1 summarizes the results. Experiment number 2 is modeled numerically except that the fall height, which is approximately between 0.29 and 0.28 m in the experiment, is specified as 0.34 m in the computational domain (= the height from the nozzle to the bottom of the container). The frequency is found to be 15.2 Hz, thus is slightly larger than those from the experiment (13.2 and 12.6Hz). This is a good agreement considering the fact that the frequency increases with increase in height (or decrease in diameter, as already determined from the basic experimental runs with a fall height of 1.7 m, where a decrease in mass flow rate led to a decrease in diameter and an increase in frequency). For most of the runs, the recording time is just a fraction of a second so that the pool does not rise enough to alter the frequency and accordingly, no change in frequency can be detected from the frame-by-frame analysis. The exception happens to be experiment number 2 (the one modeled), which is divided into 2a and 2b to account for the high and low value of fall height measured while the pool raised 1.2 cm. For this experiment, a monotonic decrease in frequency can be measured as the fall height decreases due to the rising pool. A curve fit from the experimental data to extrapolate the values to a fall height of 0.34 m gives a

projected frequency of 15.7 Hz, which puts the numerical solution (15.2 Hz) to within 4% of the expected frequency.

Another experimental run, number 6, is also modeled. The calculated frequency in this case is 44 Hz, while the experimental value is 29 Hz. The discrepancy might be due to a problem with excessive necking down of the jet in the modeling solution, which could not be resolved.

One of the basic experimental cases with a fall height of 1.7 m is also modeled. The flow rate is 20 g/s and the fluid is 60,000 cSt silicone oil. The experimental result is 190 Hz whereas the numerical result is 142 Hz. Figure 3.10 shows a sequence of oscillating flow behavior in two dimensions as obtained by the CFD simulation (Silva, 1997).

### **3.4 COMPARISON TO CRUICKSHANK AND MUNSON (1981)**

Cruickshank and Munson performed a series of experiments in 1981 that dealt with highly viscous jets impinging on a flat plate. They termed the minimum height at which the oscillations would start as the 'buckling height' and determined a maximum Reynolds number that, together with the buckling height criterion, predicted in their experiments if a jet would start to oscillate after impact on the flat surface. In addition, measurements of frequencies for various flow configurations were performed. Most results in their publication are non-dimensionalized, based on the nozzle outlet diameter and outlet velocity as well as the fall height to nozzle diameter, or  $H/d$ , ratio. Instead of mass flow rates, volumetric flow rates are employed in non-dimensionalized Reynolds numbers. Effects of inertia are neglected in the non-dimensionalization process. The main working fluid used is silicone at different nominal viscosities. Corn syrup is mentioned as another fluid used but no results are included in the publication regarding

frequencies. All comparisons made in this section refer to experimental results obtained with silicone oil. Dimensional results that are included in Cruickshank and Munson's publication has fall heights of up to 20 cm. The largest  $H/d$  ratio for which results are reported is about 100. The largest viscosity used in the results is 10,000 cSt silicone oil. Compared to the basic experiments performed in this work, both the  $H/d$  ratio (which is 140 for the basic experiments) as well as the viscosities used (12,500 cSt and higher) are for the most part significantly larger than those for Cruickshank and Munson. However, due to the experiments performed to make comparisons to computer modeling (see previous section), some of the experimental results can be compared to the Cruickshank and Munson results with the help of some minor adjustments. Also, a general comparison can be made with respect to the accuracy of the criteria developed by Cruickshank and Munson regarding the onset of oscillations. Finally, some results can be compared by performing approximate extrapolations for the non-dimensionalized results.

First, a comparison can be made regarding the general oscillating behavior for the impinging jet. Cruickshank and Munson state that the direction of oscillation is randomly distributed in their experiments. As mentioned in Section 3.2.2, the experiments performed here also show no particular trend regarding clockwise or counterclockwise coiling motion.

Second, one result presented in Cruickshank and Munson can be compared fairly well to one of the results in this work. The case at hand is silicone oil with a viscosity of 10,000 cSt, and a volumetric flow rate of 9.01 cm<sup>3</sup>/s, which translates into a mass flow rate of 8.78 g/s. These conditions are in terms of flow characteristic properties fairly close to an experiment performed by the author with 12,500 cSt silicone oil which had



a mass flow rate of 10.2 g/s. The H/d ratio for this case was 23.3. From the extrapolated graph of Cruickshank and Munson's publication, which only goes up to an H/d ratio of 20, the expected oscillation frequency should lie at about 50 Hz. The actual measured frequency is 56 Hz, which is a good match compared to Cruickshank's data, considering the number of approximations made.

Another comparison regards the criteria that Cruickshank and Munson set forth that determine if a jet will buckle upon impact. For all of their measurements, the critical H/d value lies in the vicinity of 10. The critical Reynolds number based on nozzle diameter and nozzle exit velocity is, as previously mentioned, 1.2 for axisymmetric jets. For the basic cases in this work, the H/d

criterion is easily matched ( $H/d = 140$ ). Also, the Reynolds number criterion is matched since even for the highest mass flow rate the Reynolds number at the nozzle outlet is less than 0.35. However, in at least two instances, as described in the quantitative section for silicone oil (section 3.2.2), no oscillations of any kind can be detected above a certain mass flow rate. One possibility for this discrepancy might be that inertia forces, which are neglected in Cruickshank and Munson's non-dimensionalizing process, might indeed play a role at higher physical heights H than those that are experimentally investigated by Cruickshank and Munson. Or, there might be a certain range of H/d values for which spiraling will occur and above or below which stable stagnation flow takes place.

Experiment #	Viscosity (cSt)	Fall Height (m)	Mass Flow Rate (g/s)	Uncertainty (mass flow rate)	Frequency (Hz)	Uncertainty (frequency)
1	60,000	0.33	8.8	0.007	16.7	0.09
2a	60,000	0.29	36.5	0.06	13.2	0.05
2b	60,000	0.28	36.5	0.06	12.6	0.05
4	12,500	0.315	3.5	0.003	87.4	0.7
5	12,500	0.28	10.2	0.06	56.6	0.07
6	12,500	0.28	16.5	0.04	42.1	0.03
7	12,500	0.24	24.8	0.06	29.4	0.08

**Table 3.1:** Results of Small Fall Height Experiments

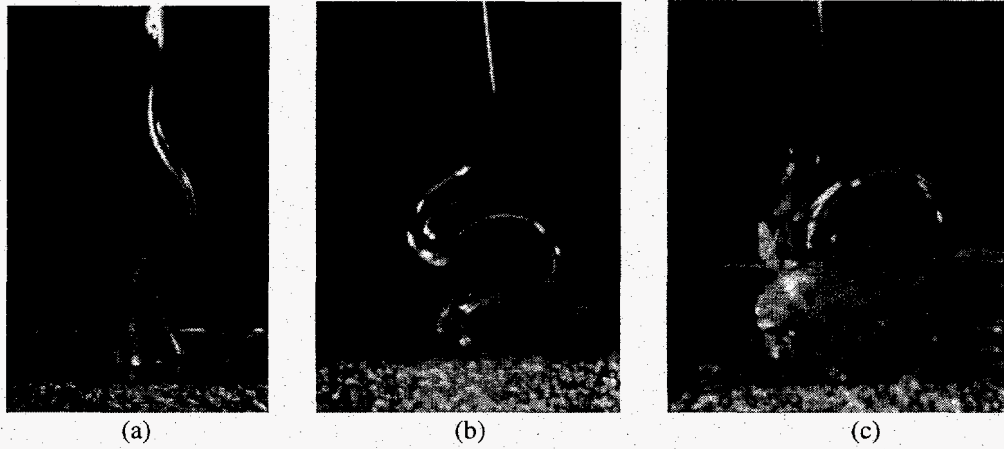


**Figure 3.1** Jet at Different Stages Upon Impact. Voids Clearly Present in the Pool.  
(a) Immediately after impact. (b) Jet folding over. (c) Spiraling starts.

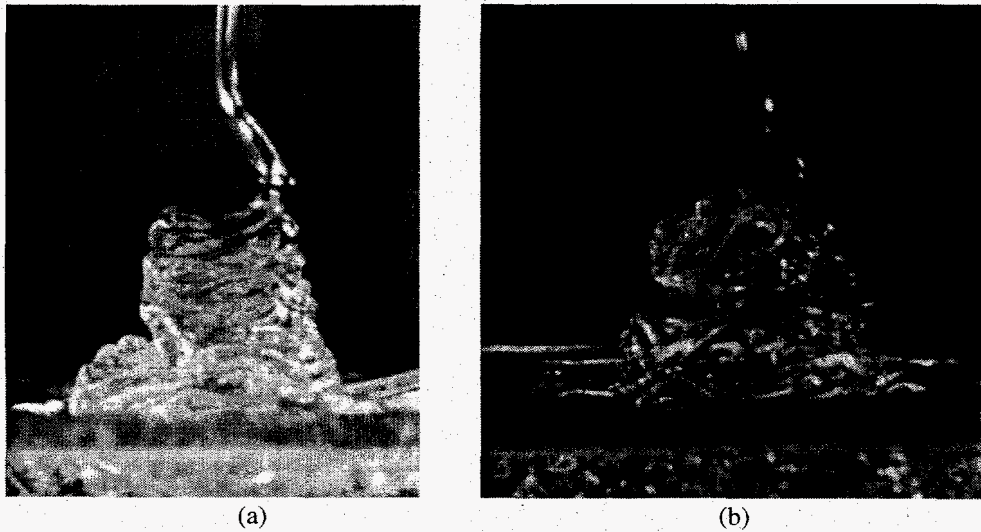


**Figure 3.2:** Jet Pile-Up at a Later Stage.  
(a) Spiraling motion. (b) Slumping to the left

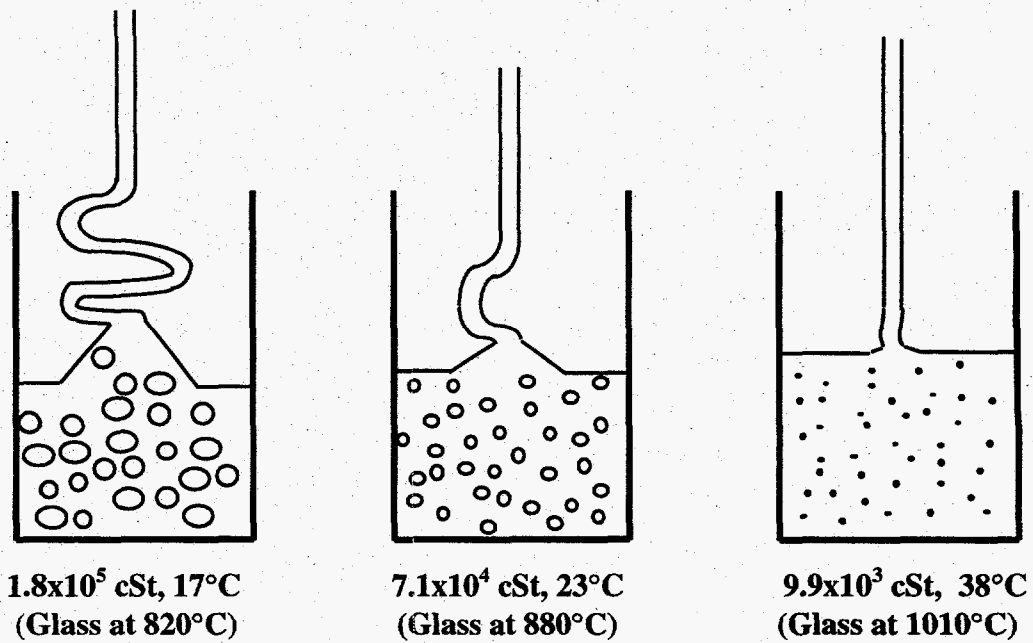


Figure 3.3 Flow Behavior of Analogous Fluid at Different Viscosities

Calculated and Measured Viscosity vs. Temperature  
for 42/43 Corn Syrup

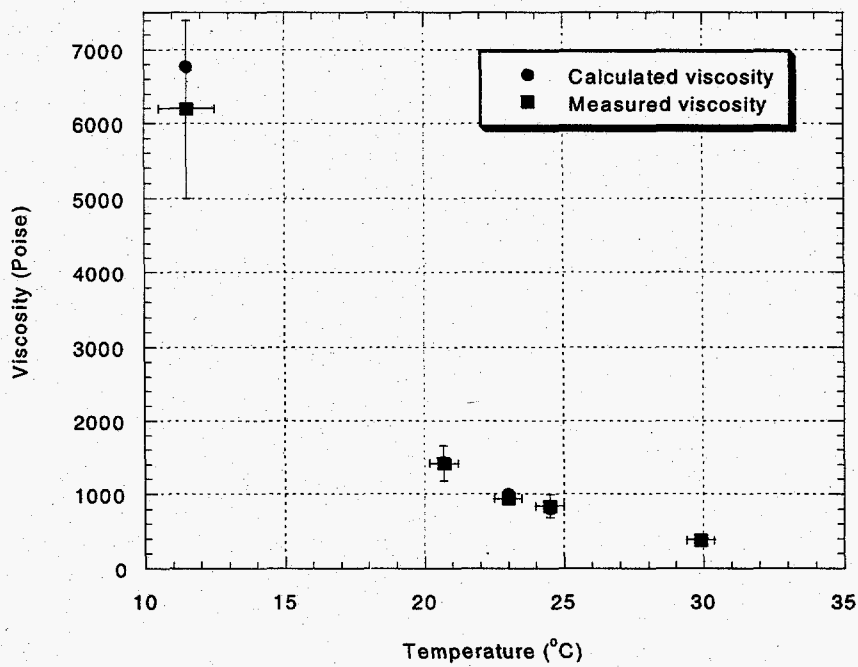
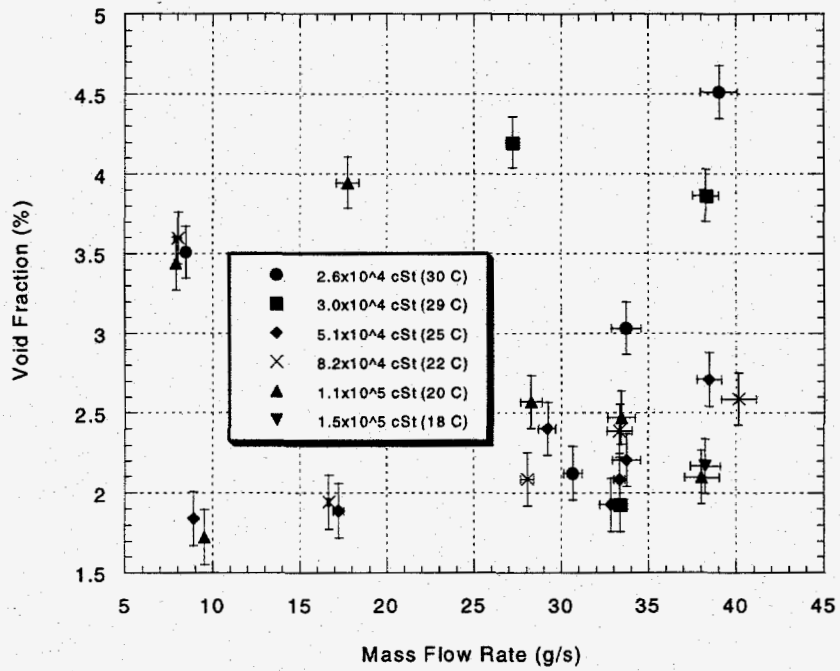


Figure 3.4: Results for Viscosity Measurements for 42/43 Corn Syrup Compared to Equation (= calculated viscosity) used by Chu and Hickox (1990)

**Void Fraction vs. Mass Flow Rate for Different Viscosities  
(Fall Height = 1.7 m, Nozzle Dia. = 12 mm)**



**Figure 3.5 Results for Void Fraction Measurements for 42/43 Corn Syrup**

**Void Fraction vs. Viscosity for Different Mass Flow Rates  
(Fall Height = 1.7 m, Nozzle Dia. = 12 mm)**

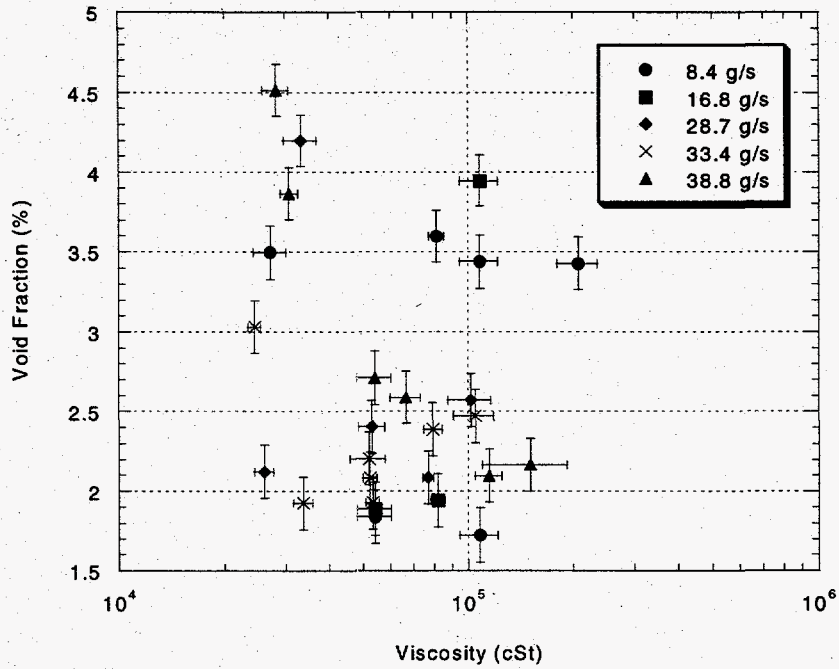


**Figure 3.6: Results for Void Fraction Measurements for 42/43 Corn Syrup**

**Frequency vs. Mass Flow Rate for 60,000 cSt Silicone Oil  
(Fall Height = 1.7 m, Nozzle Dia. = 12 mm)**

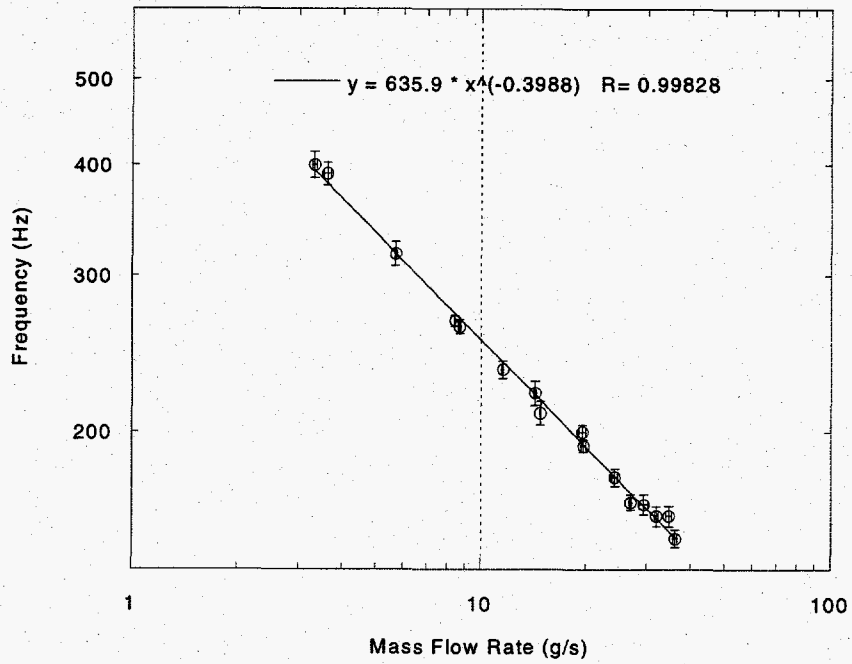


**Figure 3.7: Results of Frequency Measurements for 60,000 cSt Silicone Oil**

Frequency vs. Mass Flow Rate for 12,500 cSt Silicone Oil  
(Fall Height = 1.7 m, Nozzle Dia. = 12 mm)

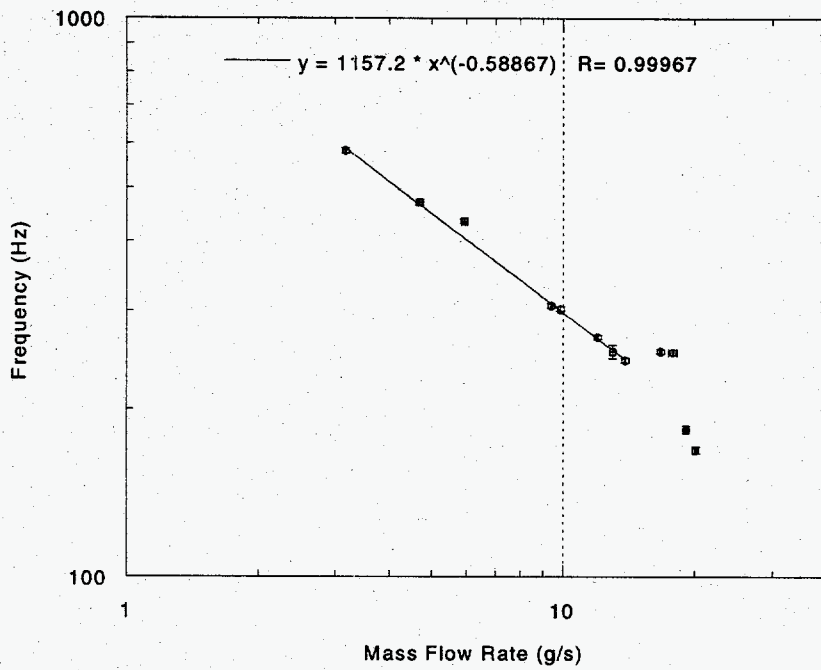
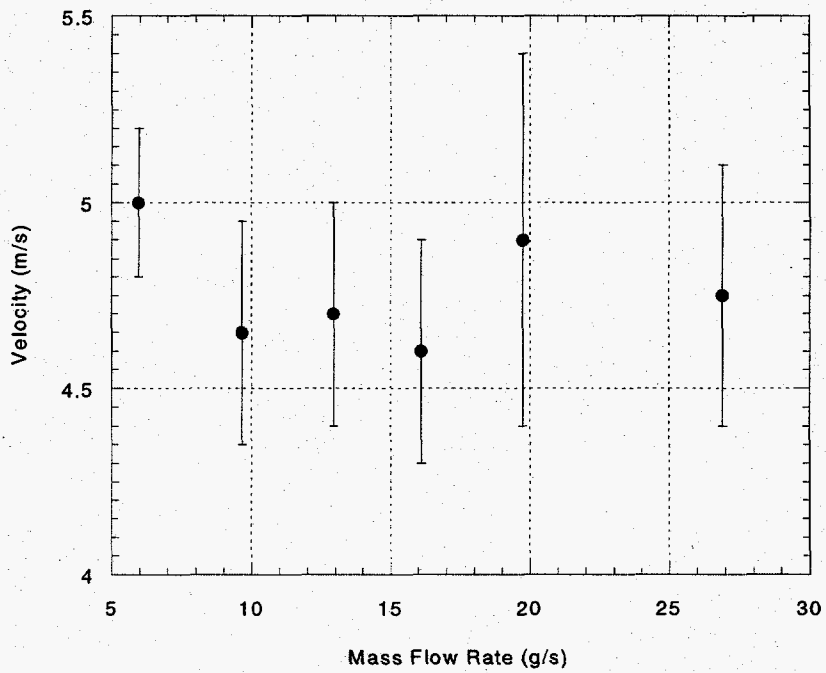


Figure 3.8: Results of Frequency Measurements for 12,500 cSt Silicone Oil

**Velocity vs. Mass Flow Rate for 60,000 cSt Silicone Oil  
(Fall Height = 1.7 m, Nozzle Dia. = 12 mm)**



**Figure 3.9:** Results for Velocity Measurements for 60,000 cSt Silicone Oil



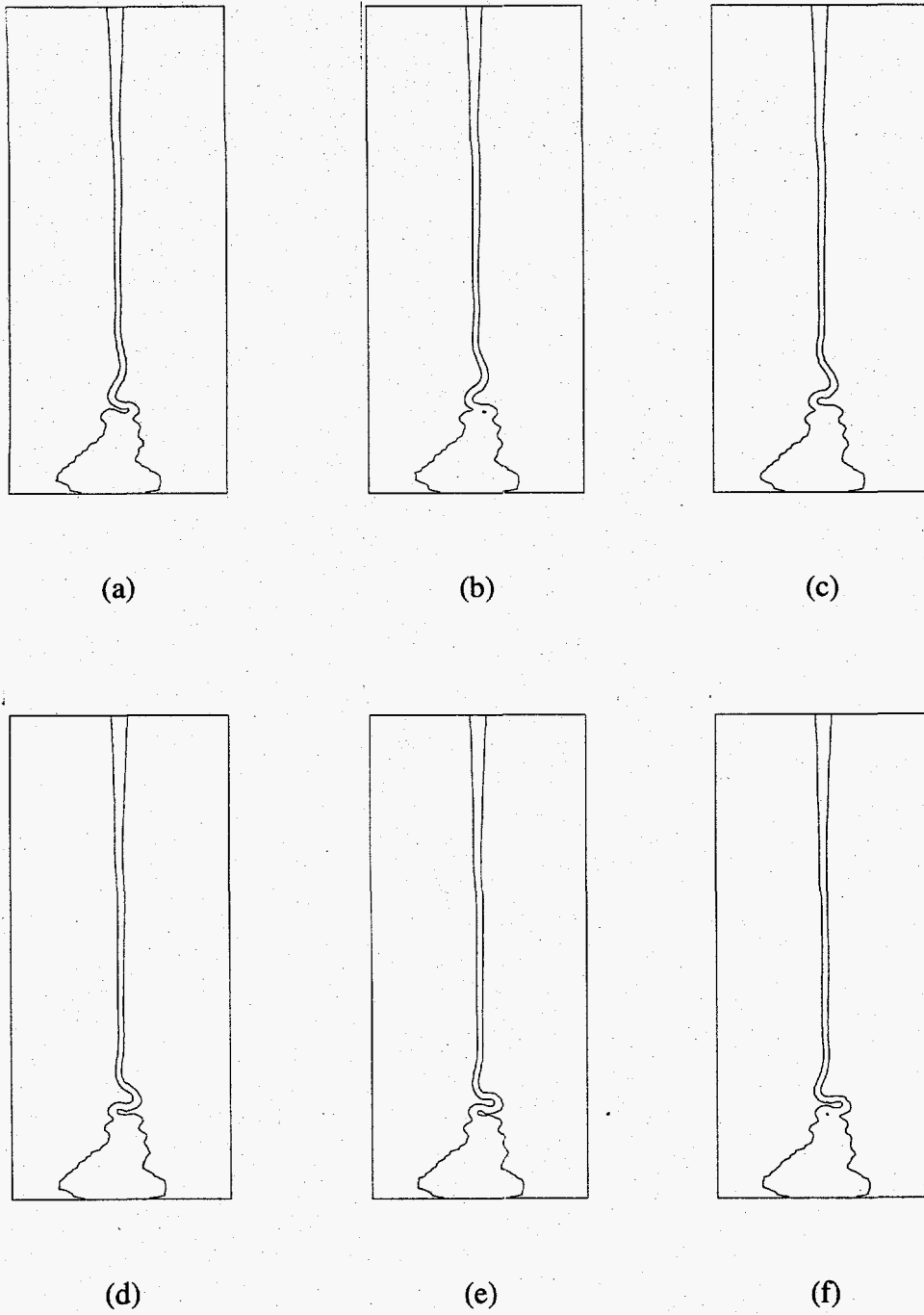


**Figure 3.10:** Sequence of Six Consecutive Frames Showing One Period of Jet Oscillation

## 4. CONCLUSIONS AND RECOMMENDATIONS

### 4.1 CONCLUSIONS

A number of qualitative and quantitative results are obtained by studying the problem of highly viscous fluid flow. A change in behavior of the fluid is observed with change in viscosity: the higher the viscosity, the higher is the degree of instability in the flow. The formation of voids can be attributed to the unstable flow behavior in the landing region. The pile-up of the fluid, which eventually leads to a slumping, causes air entrapped in the pile-up to be pushed into the fluid pool. A direct correlation between mass flow rate and/or viscosity versus void fraction cannot be established. On the other hand, all the void fractions measured are within a finite band between 1.7 and 4.5%. This means that even though an accurate prediction with a given set of parameters is not possible, the knowledge of the range in which the void fraction will fall might be sufficient, depending on the application. Of course, in light of the focus of this research, which has as one of its objectives to find a way to reduce the formation of voids, no satisfactory answer can be given at this point.

The frequency measurements yielded a good correlation of mass flow rate vs. frequency for the 60,000 cSt silicone oil. A similar correlation was found for the 12,500 cSt oil at lower mass flow rates. Different flow regimes were identified for the 12,500 cSt oil at higher mass flow rates, which led to a comparison with experiments, conducted by Cruickshank and Munson (1981). It is found that in certain cases the flow behavior is unexpected with regard to criteria for the onset of buckling set forth in Cruickshank and Munson's work.

### 4.2 RECOMMENDATIONS

#### 4.2.1 *Trial and Error*

As with probably any experimental research project, the final experimental setup often has only a scant resemblance to the initial ideas and thoughts brought into the project. Many changes are made and the acquisition of equipment leads to further modifications of the existing assembly. Also, improvements are made for those procedures that are found to be infeasible or too inefficient. Finally, experiments that are planned to be conducted initially have to be abandoned since unexpected difficulties arise which cannot be resolved or which are not practical to resolve, the cost factor always being present. In the following paragraphs a few of the ineffective approaches to experimental setup and data collection will be discussed in order to provide helpful advice for the researcher who considers the study of fluids with properties similar to the working fluids chosen by the author.

One of the most profound changes to the experimental setup was made (unfortunately) after data had already been collected for a few months. The task of getting rid of air bubbles in the working fluid before filling the cylinder and ensuring that the fluid stays bubble-free during the filling process or that the air bubbles are removed after the hydraulic cylinder is filled started out as a very tedious and time-consuming activity which also caused considerable wear and tear on the experimental assembly. The hydraulic cylinder was first filled with the working fluid, leaving a considerable amount of air bubbles inside the cylinder (as could easily be verified by test pours of the untreated cylinder). This was done in the vertical position, the cylinder being attached to a separate wooden board. The fluid (at that time corn syrup) was filled hot (45°C) to accelerate the escape of the air bubbles through the nozzle, which was left open to the

atmosphere. This process took 2 days where the fluid was kept warm by constantly circulating hot water from a temperature bath through tubing around the cylinder. The cylinder then had to be unmounted from the wooden board and mounted back onto the main board with the motor and traversing mechanism. Since the fluid was still relatively warm, the working fluid had to be left under the environmental control of the constant temperature baths for up to three days, depending on the required viscosity for the experimental run planned. Thus, a total of up to 5 days passed before one experimental run was conducted. A new approach to the problem was made by extending the nozzle system of the hydraulic cylinder and attaching a 19-liter bucket to the end of it. Care had to be taken that all connecting parts were sealed properly. One translucent section was added to the nozzle system to allow for visual inspections to make sure that no air bubbles entered the cylinder, which was now filled by slowly retreating the piston and thus pulling the fluid directly from the bucket through the nozzle system. Since the bucket can hold up to 19 liters, 4 to 5 experiments could be run consecutively before the bucket had to be refilled and the fluid became bubble free in one to two days due to the much larger surface area exposed to the environment. This cut down on the waiting time from 5 days to an average of 1 1/2 days. According to Cruickshank and Munson's schematic of their experimental setup and the author's experience with silicone oil, the formation of voids in the fluid pool below the plate onto which Cruickshank and Munson had the fluid dropped must have been unavoidable. Furthermore, since the fluid was "recycled" by being pumped back to the nozzle outlet for additional experiments, the presence of voids in consecutive experiments was virtually guaranteed. Cruickshank and Munson mention the presence of bubbles in the fluid but do not describe how the problem was

handled satisfactorily, except that higher viscosities were avoided.

One of the initial measurements planned that had to be abandoned eventually was to determine the jet diameter by using a shadowgraph from a laser sheet. Numerous trials to determine the diameter, which lies in the millimeter range, failed due to lack of appropriate optical equipment. The shadow thrown from the lens which sent the laser's beam through the jet was too small to be resolved accurately. In addition, the shadow itself could not be brought into "focus" which rendered it impossible to determine the outline of the jet on the shadow graph.

With the acquisition of the high-speed camera the problem could be partially and indirectly solved. The velocity measurements together with mass flow rate measurements made it possible to determine the diameter of the jet in the landing region. However, as mentioned earlier, the uncertainty in the velocity measurements is comparatively large so that an exact measure of the diameter could still not be obtained. Due to some discrepancies with the results compared to Cruickshank and Munson, the issue of non-dimensionalizing the results based on nozzle outlet conditions was rendered questionable and the inability to accurately measure either the velocity or the diameter in the landing region of the jet prevented a localized non-dimensionalizing approach.

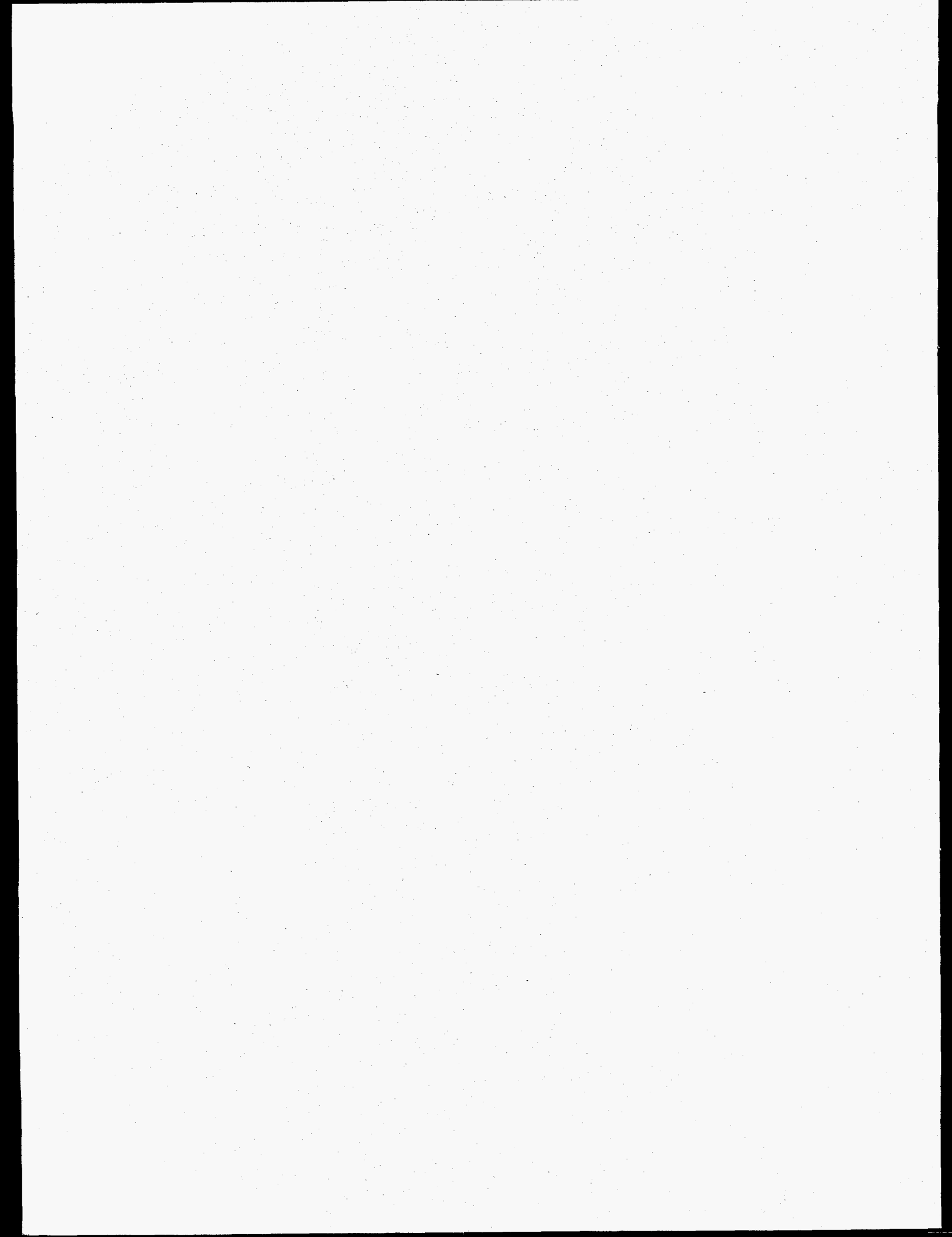
Another series of experiments that had to be abandoned was the void fraction measurement of silicone oil. The use of water as the fluid into which the oil is submerged was not pursuable since silicone oil is slightly less dense. A different fluid tried was ethanol. Although the silicone oil could be immersed into ethanol, air bubbles on or right beneath the silicone oil surface carried immediately a layer of silicone oil to the free surface which caused the measurement to be invalid.

#### 4.2.2 *Future Work*

More experimental data need to be collected to complete the picture for both working fluids used. For corn syrup, additional experiments need to be conducted to further investigate the issue of repeatability of measurements. Due to time constraints only very few data points have been repeated and the result is inconclusive. If indeed, as the present results suggest, the void fraction is not a function of the parameters chosen for the experiments, a more extensive collection of repeated measurements should reveal that the void fraction is not a function of the selected parameters, at least not in the range and/or resolution that could be realized in the experiments. As for the correlation found for the highest mass flow rate chosen, additional measurements should be performed as well to either validate the result or discard the possibility of a correlation.

Possibly a large-scale experiment that comes closer to the actual "Can-in-Canister" assembly might result in better predictions of what void fraction will be present under certain parametric conditions.

As for the silicone oil experiments, it seems that further investigations into the issues of buckling criteria will yield useful contributions to the topic, in particular regarding the fact that no other relevant experimental research has been conducted (to the knowledge of the author) since Cruickshank and Munson's experiments in 1981.



## REFERENCES

1. Amarillo National Resource Center for Plutonium (1996). *Fiscal Year 1997: Continuation Application (abbr. ver.) for the Amarillo National Resource Center for Plutonium*.
2. Beckwith, T. G., & Marangoni, R. D. (1990). *Mechanical Measurements*. 4<sup>th</sup> ed. New York: Addison-Wesley.
3. Bejan, A. (1987). Buckling flows: a new frontier in fluid mechanics. *Annual Review of Numerical Fluid mechanics and Heat Transfer*, 1, 262-304.
4. Buckmaster, J. (1972). The buckling of thin viscous jets. *Journal of Fluid Mechanics* 61, 449-463.
5. Chu, T.Y., & Hickox, C.E (1990). Thermal convection with large viscosity variation in an enclosure with localized heating. *Journal of Heat Transfer* 112, 388-395.
6. Cruickshank, J.O., & Munson, B.R. (1981). Viscous fluid buckling of plane and axisymmetric jets. *Journal of Fluid Mechanics*, 113, 221-239.
7. Cruickshank, J.O. (1987). Low-Reynolds-number instabilities in stagnating jet flows. *Journal of Fluid Mechanics*, 193, 111-127.
8. Fox, R.W. & McDonald, A.T. (1992) *Introduction to Fluid Mechanics*. 4<sup>th</sup> ed. New York: John Wiley & Sons.
9. Jerrell, J.W. & Hardy, B.J. (1995). Estimates of Glass Temperatures and Viscosities During Filling of Can-in-Canister Assembly. *Savannah River Technology Division, Westinghouse Savannah River Company*.
10. Kline, S.J., & McClintock, F.A. (1953). Describing Uncertainties in Single-Sample Experiments. *Mechanical Engineering*, 75, 3-8.
11. National Academy of Sciences, 1994, *Management and Disposition of Excess Weapons Plutonium*, Washington, D.C.: National Academy Press.
12. Plodinec, M.J. (1987), SGM Run 8 - Canister and glass temperatures during filling and cooldown. *Technical Division, Savannah River Laboratory*.
13. Silva, M.W. (1997). *A Computational Study of Highly Viscous Impinging Jets*. Thesis. The University of Texas at Austin.
14. Soper, P.D., & Bickford, D.F. (1982). Physical Properties of Frit 165/Waste Glasses DPST-82-899. *Technical Division - Savannah River Laboratory, Aiken, SC*.
15. Suleiman, S.M. & Munson, B.R. (1981). Buckling of a thin sheet of a viscous fluid. *Phys. Fluids*, 24, 1-5.
16. Taylor, G.I. (1968). Instability of jets, threads, and viscous sheets. *Proceedings of the 12<sup>th</sup> International Congress of Applied Mechanics* (pp. 382-388), Stanford.
17. Tchavdarov, B., Yarin, A.L, & Radev, S. (1993). Buckling of thin liquid jets. *Journal of Fluid Mechanics*, 253, 593-615.
18. Tipler, P.A. (1991). *Physics for Scientists and Engineers: Volume 1*. 3<sup>rd</sup> ed New York: Worth Publishers.
19. Viskanta, R. (1994). Review of three-dimensional mathematical modeling of

glass melting. *Journal of Non-Crystalline Solids*, 177, 347-362.

20. Zak, M. (1985). Shape instability in thin viscous films and jets. *Acta Mechanica*, 55, 33-50.